Degradation and mineralization of antipyrine by UV-A LED photo-Fenton reaction intensified by ferrioxalate with addition of persulfate

Degradation and Mineralization of Antipyrine by UV-A LED Photo-Fenton Reaction Intensified by Ferrioxalate with Addition of Persulfate

Konstantina Davididou[a], José María Monteagudo[b,*], Efthalia Chatzisymeon[a], Antonio. Durán[b], Antonio José Expósito[b]

[a] *Institute for Infrastructure and Environment, School of Engineering, The University of Edinburgh, Edinburgh EH9 3JL, United Kingdom.*

[b] *Department of Chemical Engineering, Grupo IMAES, Escuela Técnica Superior de Ingenieros Industriales, Instituto de Investigaciones Energéticas y Aplicaciones Industriales (INEI) University of Castilla-La Mancha, Avda. Camilo José Cela 3, 13071 Ciudad Real (Spain).*

* To whom correspondence should be addressed

Fax: 0034 926295361.
Phone: 0034 926295300, ext: 3888
email: josemaria.monteagudo@uclm.es

ABSTRACT

The intensification of the degradation of antipyrine in aqueous solution by using a UV-A-LED-photo-Fenton reaction intensified by ferrioxalate complexes and with addition of persulfate anions was studied. The efficiency of the reaction was evaluated in terms of antipyrine degradation and mineralization degree at different initial concentrations of hydrogen peroxide, ferrous ion, oxalic acid and persulfate anion. The reaction was carried out using a lab-scale photoreactor irradiated with artificial UV-A-LED light emitting at 365 nm. Artificial neural networks (NNs) were implemented for modelling the degradation process. Under optimal conditions, complete degradation of antipyrine and 93% mineralization was reached in 2.5 and 60 min, respectively. The contribution of $HO^{\bullet}$ radicals in this system was evaluated running the reaction in the absence and presence of appropriate quenchers such as tert-butyl alcohol and methanol. In the last step of reaction, possibly different intermediates such as 2-butenedioic acid, butanedioic acid, 4-oxo-pentanoic acid, acetate and formate can be generated which cannot be degraded by $HO^{\bullet}$ radicals or their reaction is very slow. This ferrioxalate-mediated system reduces the amount of H_2O_2 needed (100 mg L^{-1}) for antipyrine degradation and persulfate was not necessary because it could not be activated with UV-A LED nor with Fe^{2+} since it is quickly converted to Fe^{3+} forming ferrioxalate complexes.

Keywords: antipyrine; UV-LED; persulfate; ferrioxalate; pharmaceuticals; modelling

1. INTRODUCTION

The consumption of pharmaceuticals compounds in last years has increased considerably leading to the increase in their concentration in urban wastewaters [1- 3]. These compounds are known to be recalcitrant to biodegradation because of their aromatic structure and their low solubility in water. So, they are only slightly degraded in sewage wastewater treatment plants [4, 5]. For instance, antipyrine is a pharmaceutically active compound detected in various natural environments [6, 7]. The percentage of removal of antipyrine in effluents from conventional wastewater treatment plants is only about 30% [8]. Therefore, an effective tertiary treatment for the removal of antipyrine would be necessary.

Advanced Oxidation Processes (AOPs) are being proposed as valuable approaches for pharmaceuticals pollutants wastewater treatment. It is well-known that the efficiency of AOPs is based on the generation of highly reactive free radicals such as hydroxyl radicals ($HO^{\bullet}$, E_o= 2.8 V) or sulfate radicals ($SO_4^{\bullet -}$, E_o= 2.6 V). $HO^{\bullet}$ can be generated by various combinations such as UV/H_2O_2, Fenton, photo-Fenton, ferrioxalate-based systems, UV/TiO_2, UV/O_3 or these processes in conjunction with ultrasound. Sulfate radicals can be formed in AOPs based on systems with activated $S_2O_8^{2-}$ by UV light, transition metals, hydrogen peroxide or ultrasound [9].

Several processes including direct photolysis and UV/H_2O_2 [10, 11], Sono-photo-Fenton [12], ferrioxalate-assisted solar photo-Fenton [12-14] have been investigated for the removal of antipyrine.

Oxidation of antipyrine aqueous solution by UV-C/ $S_2O_8^{2-}$ [11] or by heat activated persulfate [15] has also been reported in the scientific literature. The effectiveness of these studies was examined in terms of antipyrine removal, but they have not reported data about mineralization.

However, until now, UV-A LED lamps have not been used for the degradation of antipyrine in AOPs. LEDs offer potential advantages over conventional UV lamps like high efficiency, compactness, lower energy consumption, robustness, not overheating, long life times, no disposal problems and no warm-up time [16, 17]. LEDs are semiconductor p-n junction diodes, which, when activated, emit light due to electrons and holes recombination (i.e. electroluminescence). Recombined electrons and holes become more stable and release excess energy by emitting photons of the same frequency. A key advantage of LEDs is that almost all electrical energy can be converted into monochromatic light energy [16]. The light output is linearly proportional to the current within its active region, so the light output can be precisely modulated to send an undistorted signal through a fiber optic cable. A LED is a directional light source, with the maximum emitted power in the direction perpendicular to the emitting surface [18].

The main objective of the present work was to optimize the degradation and mineralization of an antipyrine aqueous solution by using a UV-A LED photo-Fenton system using a LED lamp with a light peak emission wavelength at 365 nm. The intensification of this photo-Fenton system with ferrioxalate was studied as it is a photo-sensitive complex being 320-400 nm irradiation favorable for the ferrioxalate photochemistry [19-20].

Additionally, the photolysis of ferrioxalate generates more H_2O_2 which, with Fe(II), yields more $HO^{\bullet}$ radicals through the well-known Fenton reaction mechanism [21,22], improving the degradation process. The addition of persulfate was also studied to test the synergistic effect of its possible activation with ferrous ion and hydrogen peroxide in this UV-A LED photo-Fenton process.

Experimental tests based on a Factorial Design were analyzed and results were fitted using neural networks (NNs), which allowed the value of the Response Functions (degradation of antipyrine or mineralization degree (mg L^{-1} TOC removed)) to be estimated within the studied range as a function of the operating variables (1: initial concentration of hydrogen peroxide, 2: initial concentration of Fe^{2+}, 3: initial concentration of oxalic acid, 4: initial concentration of persulfate). The effects of the variables on Response Functions were also determined.

Finally, the reaction kinetics and hydroxyl and sulfate radical contribution on the mineralization reaction were also studied.

2. EXPERIMENTAL

2.1. Materials and chemicals

Antipyrine, $C_{11}H_{12}N_2O$ (99%) (Fig. 1) was obtained from Acros. $FeSO_4 \cdot 7H_2O$, sodium persulphate ($Na_2S_2O_8$, 98%), oxalic acid ($H_2C_2O_4.2H_2O$, 99.5%) and tert-butyl alcohol were purchased from Panreac. Hydrogen peroxide (30% w/v) was obtained from Merck. Methanol was obtained from Sigma-Aldrich. All chemicals were used as received without further purification.

The initial concentration of antipyrine was always 50 mg L^{-1} (TOC= 35 mg L^{-1}). For experimental runs focused on the evaluation of radical mechanism, tert-butyl alcohol and methanol were added to the system as radical scavengers [23].

Figure 1

2.2. UV-light emitting diodes (UV-A LED)

The UV LED photosystem was developed with an indium gallium nitride (InGaN) LED lamp (LZ4-00U600 LED ENGIN, USA) with a light peak emission wavelength at 365 nm (see Fig. S1, Supplementary Material). The nominal consumption of the LED lamp was 1.80 W, for an applied current of 700 mA. The photon flux emission of UV-A-LED was determined by potassium ferrioxalate actinometer and found to be 3.32×10^{-6} Einstein s^{-1}.

2.2. UV-A LED photocatalytic reactor

The schematic diagram of the experimental system employed in this research is shown in Fig. 2. A quartz protective plate is placed between the reactor and the UV-LED lamp emitting at 365 nm. The volume of the reactor is 150 mL.

All experiments were carried out in a batch mode lab-scale photoreactor illuminated with a UV-A LED lamp.

Figure 2

2.2. Experimental procedure

The experiments were carried out in the batch UV-A LED photoreactor indicated above. The pH was adjusted to 2.8 with H_2SO_4 and NaOH solutions to avoid iron precipitation. Then, $FeSO_4.7\ H_2O$, oxalic, hydrogen peroxide and persulfate were directly added to the photoreactor at the beginning of each experiment. All the experiments were run at room temperature between 24 and 26 ºC. For the duration of the tests, the samples were periodically withdrawn from the reactor to obtain the residual concentrations of antipyrine, total organic carbon (TOC), ferrous iron, hydrogen peroxide, persulfate and dissolved oxygen.

Hydroxyl radical scavenging was accomplished using 1 M tert-butyl alcohol or methanol to determine the contributions of the radical reactions to mineralization. Before analysis, all samples were withdrawn from the reactor to determine their H_2O_2 contents and were immediately treated with excess Na_2SO_3 (in solution) to prevent further oxidation (this procedure was performed to avoid overestimating degradation).

2.3. Analysis

Analysis of antipyrine concentration was carried out by high-performance liquid chromatography with UV detection (Agilent Technologies 1100 HPLC-UV) in isocratic mode immediately after sampling. An Eclipse XDB-C18 column (5 μm, 4.6 × 250 mm) was used with an 60:40 (v/v) methanol/(water with 0.1% acetic acid) mixture at acidic pH as the mobile phase (detection wavelength, λ= 286 nm; flow rate of 0.6 ml min^{-1}).

The mineralization degree of treated wastewater was determined using a TOC analyzer (TOC-5050 Shimazdu, standard deviation < 0.2 mg L^{-1}). The H_2O_2 content in solution was determined by Quantofix peroxide test strips (Sigma-Aldrich). The concentration of soluble iron species during the mineralization reaction was measured spectrophotometrically with 1,10-phenanthroline (according to ISO 6332) using a UV-Vis spectrophotometer (HACH LANGE). Determination of residual $S_2O_8^{2-}$ concentrations in the presence of iron was performed according to the method of Liang et al. [24]. Dissolved oxygen concentration was measured using a Jenway 9200 DO_2 meter. Experiments were conducted in triplicate and standard error was found to be approximately 5%.

2.4. Experimental design

A Central-Composite Experimental Design was applied to investigate the effects of four variables (1: initial concentration of hydrogen peroxide, 2: initial concentration of Fe^{2+}, 3: initial concentration of oxalic acid, 4: initial concentration of persulfate) on the chosen Response Functions (degradation of antipyrine and mineralization degree (mg L^{-1} TOC removed). The process design consisted of three series of experiments (Table 1):

(i) a factorial design with 2^k trials (all possible combinations of codified values +1 and –1), which in the case of k = 4 variables consisted of 16 experiments (1-16)

(ii) selection of the axial distance of the star points (codified values $\alpha = 2^{k/4} = \pm 2$) consisting of 2k = 8 experiments (experiments 17-24), and

(iii) replicate of the central point (three experiments, 25-27).

The complete experimental design and additional experiments, including variable ranges and obtained Response Functions values, are also shown in Table 1.

Table 1

2.5. Neural-network strategy

The neural network applied in this work was solved with two neurons, using a simple exponential activation function and a solution strategy based on a back-propagation algorithm [25, 26]. Parameters were fitted using the Solver tool in a custom spreadsheet in Microsoft Excel using a nonlinear fitting method. The input variables in this study were 1) initial concentration of hydrogen peroxide, 2) initial concentration of Fe^{2+}, 3) initial concentration of oxalic acid, 4) initial concentration of persulfate. The chosen response functions were A) degradation of antipyrine and B) mineralization degree (mg L^{-1} TOC removed). The effects of the studied variables on the response functions were also evaluated. Finally, a measure of the saliency of the input variables was made based on the connection weights of the neural networks. This study analyzed the relevance of each variable with respect to the others (expressed as percentages).

3. RESULTS AND DISCUSSION

3.1 Preliminary study

An initial comparative study on the degradation of 50 mg L^{-1} antipyrine aqueous solution at pH 3 under different single systems such as UV-A-LED, H_2O_2 or $S_2O_8^{2-}$ was done. Taking into account the results, we could conclude that the antipyrine degradation via direct photolysis using UV-A-LED light was very inefficient (5%). On the other hand,

hydrogen peroxide or persulfate anion alone insignificantly affected the degradation of the antipyrine which confirmed that the direct or molecular reactions between these oxidant species and the possible compounds present in the antipyrine solution did not occur or had slow oxidative kinetics. In these single systems, possible oxidative intermediate species (mainly hydroxyl radicals) were not generated either.

Taking into account the results from this preliminary study, a central-composite experimental design was applied to optimize the ferrioxalate-induced photo-Fenton process under UV-A-LED and with addition of persulfate, as this catalytic system could offer a practical alternative for the destruction of this type of contaminants.

3.2 Ferrioxalate system kinetics evaluation

In the ferrioxalate assisted UV-A-LED photo-Fenton reaction with persulfate addition, the antipyrine degradation followed pseudo-first-order kinetics with respect to the antipyrine concentration, as follows:

$$-r = -\frac{dC_{AP}}{dt} = k_{AP} C_{AP} \quad (1)$$

where r is the reaction rate, C_{AP} is the concentration (mg L^{-1}) of antipyrine at a given time, t (min) and k_{AP} is the pseudo-first-order degradation rate constant (min^{-1}). This equation can be integrated between $t = 0$ and $t = t$, yielding:

$$\ln \frac{C_{AP}}{(C_{AP})_o} = -k_{AP} t \quad (2)$$

where $(C_{AP})_o$ is the initial concentration of antipyrine. According to this expression, a plot of the first term versus "*t*" must yield a straight line satisfying Eq. (2) with slope k_{AP}.

252

253 **3.3. NNs fitting**

254

255 The experimental results obtained for the response functions [A) pseudo-first-order
256 kinetic rate constant of antipyrine degradation (k_{AP}, min^{-1}) and B) %TOC removal of
257 antipyrine aqueous solution] under the UV-A LED photo-Fenton process intensified with
258 ferrioxalate and with addition of persulfate (shown in Table 1) were fitted with NNs,
259 resulting in an average error of less than 15% in both cases. The equation and fitting
260 parameters are shown in Table 2. N1 and N2 are general factors related to the first and
261 the second neurons, respectively. W11 to W14 are the contribution parameters to the first
262 neuron and represent the influence of each of the four variables in the process: 1) initial
263 concentration of hydrogen peroxide, 2) initial concentration of Fe2+, 3) initial
264 concentration of oxalic acid, 4) initial concentration of persulfate, respectively. W21 to
265 W24 are the contributions to the second neuron corresponding to the same variables.

266 Table 2

267 The results of a saliency analysis on the input variables for each neural network
268 (%) are also shown in Table 2. From these results, it was possible to deduce the effect of
269 each parameter on the response function. Thus, it was confirmed that both the antipyrine
270 degradation and the mineralization of solution under the UV-A LED photo-Fenton
271 process intensified by ferrioxalate and with addition of persulfate process was mainly
272 influenced by the initial concentration of persulfate (although with negative effect) and
273 by the initial concentration of the catalyst Fe^{2+} (positive effect), as will be explained
274 below.

275

3.4. Antipyrine degradation and mineralization study

Equation and parameters shown in Table 2 enabled a simulation analysis of the effects of the studied variables on the value of the two chosen Response Functions, 1) the pseudo-first-order kinetic rate constant of antipyrine degradation (k_{AP}) and 2) %TOC removal. Figs. 3 and 4 show the effects of the four variables (initial concentrations of hydrogen peroxide, Fe^{2+}, oxalic acid and persulfate) on k_{AP} and TOC removal, respectively. Figs. 3abc and 4abc show results corresponding to center point operating conditions and Figs. 3d and 4d show results that would be obtained under the selected optimal conditions using NNs.

It was found that both Fe^{2+} and oxalic had a positive effect on both k_{AP} and %TOC removal over the studied range. This could be due to the continuous regeneration of Fe^{2+} via photoreduction of Fe^{3+} with 365 nm UV-A-LED light and generation of hydroxyl radicals according to Eqs. (3) and (4):

$$Fe^{3+} + H_2O \rightarrow Fe^{3+}(OH)^{2+} + H^+ \quad (3)$$

$$Fe^{3+}(OH)^{2+} + h\nu \rightarrow Fe^{2+} + HO^{\cdot} \quad (4)$$

Ferric ions were formed by the oxidation of ferrous ion (added as $FeSO_4$) by dissolved oxygen (Eq. (5)) and by Fenton reaction (Eq. (6)) also generating superoxide radical anion and hydroxyl radicals as follows:

$$Fe^{2+} + O_2 \rightarrow Fe^{3+} + O_2^{\cdot -} \quad (5)$$

$$Fe^{2+} + H_2O_2 \rightarrow Fe^{3+} + HO^{\cdot} + OH^- \quad (6)$$

On the other hand, ferrioxalate is formed *in situ* by reaction between oxalic acid and Fe^{3+} as indicated in Eq.(7) and extra hydroxyl radicals are generated by ferrioxalate photochemistry as previously reported [27].

$$Fe^{3+} + H_2C_2O_4 \rightarrow [Fe^{3+}(C_2O_4)_3]^{3-} + 6H^+ \quad (7)$$

Figs. 3d and 4d show that both the antipyrine degradation constant (k_{AP}) and mineralization degree (%TOC removal) increased with the $[H_2C_2O_4]$/[Fe] molar ratio up to 3, because at an $[H_2C_2O_4]$/[Fe] molar ratio of 3, the Fe^{3+} ions were complexed with the maximum amount of oxalate, in the form of the saturated complex $Fe(C_2O_4)_3^{3-}$ (ferric complexed with three oxalate molecules as its limit load). As it can be seen in Figs. 3d and 4d, the optimal $[H_2C_2O_4]$/[Fe] molar ratio is 100 mg L^{-1} $H_2C_2O_4$/20 mg L^{-1} Fe <> 1.11 mM $H_2C_2O_4$/0.36 mM Fe (≈ 3). However, when the molar ratio is below 3, insufficient oxalate amount is present, and some of the ferric ions can precipitate as $Fe(OH)_3$, reducing the yield of Fe^{2+} ion regeneration. An excess of oxalate could act as an additional organic compound and so compete the $HO^{\bullet}$ radicals with antipyrine and intermediates reducing the mineralization efficiency.

However, as it is shown in Figs. 3a and 3c, the optimal initial concentration of hydrogen peroxide over the studied range was the minimal value, 100 mg L^{-1}. In a preliminary study using H_2O_2 concentrations below this value lower k_{AP} values were obtained (see Table S1, Supplementary Material). This could be justified because ferrioxalate photochemistry provides extra sources of oxidant H_2O_2 and catalyst Fe^{2+} for the Fenton reaction to yield more $HO^{\bullet}$ radicals [27, 28]. It is well-known that an increase in H_2O_2 concentration produces a higher amount of $HO^{\bullet}$ radicals by Fenton reaction. However, an excess of hydrogen peroxide reduces catalytic activity since it favours

reaction (8) with a very high kinetic constant, k= 4.7 10^7 M^{-1} s^{-1}, (where $HO^{\bullet}$ reacts with peroxide), reducing the amount of radicals available to destroy antipyrine and producing the well-known *scavenger effect*.

$$H_2O_2 + HO^{\bullet} \rightarrow HO_2^{\bullet} + H_2O \quad (8)$$

Although other radicals ($HO_2^{\bullet}$) are produced, their oxidation potential is much smaller than that of the hydroxyl radicals. Additionally, decomposition of hydrogen peroxide to form water and oxygen is also favoured by Eqs (8) and (9).

$$HO^{\bullet} + HO_2^{\bullet} \rightarrow H_2O + O_2 \quad (9)$$

As shown in Figs. 3c, 3d, 4c and 4d, an increase in the concentration of oxalic acid, up to 100 mg/L, resulted in a significant positive effect on antipyrine degradation (Figs. 3c and 3d), while this increase merely affected process efficiency in terms of intermediates' mineralization (Figs. 4c and 4d). These findings indicate that oxalic acid addition plays an essential role during the first step of the degradation reaction, when antipyrine oxidation takes place. Antipyrine was always totally degraded in less than 15 min. It was also reflected in the salience analysis (%) shown in Table 2.

With respect to the effect of persulfate on reaction, we can see in Figs. 3a and 4a that it has a negative effect on both the antipyrine degradation constant and mineralization degree practically in the overall studied range. This demonstrated that no persulfate activation took place possibly due to two reasons: (a) the UV-A LED lamp emitted at 365 nm while persulfate absorbs light below 288 nm and so it could not be activated with UV-A LED, and (b) persulfate was not activated by Fe^{2+} either, due to the fast conversion of ferrous into ferric and formation of ferrioxalate complexes. On the other hand, when initial persulfate concentration increased, the *scavenger effect* capturing hydroxyl radical

increased according to Eq (10) [29] decreasing the availability of $HO^{\bullet}$ and so the degradation eficacy. So, persulfate was not neccesarily used in this ferrioxalate-photochemistry-based system.

$$S_2O_8^{2-} + HO^{\bullet} \rightarrow S_2O_8^{\bullet-} + OH^- \qquad (k= 1.4 \times 10^7\ M^{-1}\ s^{-1}) \qquad (10)$$

3.5. Reaction analysis

Fig. 5 shows the evolution of antipyrine, TOC and dissolved oxygen concentrations along the reaction (average values of three replicated experiments) under the optimal operating conditions selected by Factorial Design and NNs. Under these conditions ($[H_2O_2]_o$= 100 mg L^{-1}, $[Fe^{2+}]_o$= 20 mg L^{-1}, $[H_2C_2O_4]_o$= 100 mg L^{-1}, $[S_2O_8^{2-}]_o$= 0 mg L^{-1}, temperature= 24-26ºC, pH= 2.8) antipyrine was fully degraded in 2.5 min and 93% TOC removal was achieved in approximately 60 min. It was observed that mineralization degree reached in the presence of UV-LED was higher than that obtained in our previous study on antipyrine degradation using the ferrioxalate-assisted solar photo-Fenton process under optimal conditions (83% TOC removal in 60 min). A comparison of the two alternative processes is difficult because the irradiation sources and used reactors geometry are different. The higher efficiency of the UV-LED system may be attributed to the fact that UV-LED system emits monochromatic irradiation at 365 nm, which is very close to the maximum absorbance wavelength of ferrioxalate complexes (see Fig. S2, Supplementary Material). The value of the pseudo-first-order kinetic rate constant of antipyrine degradation, k_{AP}, calculated from the results in optimal conditions was 1.50 min^{-1}. This was the value predicted by the model shown in Fig. 3d. However, the mineralization

degree obtained, 93%, was different than the model predicted (≅99%) shown in Fig. 4d. It could be explained because the mathematic model did not take into account the possible formation of intermediates refractory towards hydroxyl radicals and subsequently stop of mineralization reaction. As it is shown, TOC abatement curve corresponding to the intermediates degradation linearly decreased during the first 15 min while it only slightly decreased and remained constant above around 25 min being 93% TOC removal attained (Final concentration of TOC= 6 mg L^{-1}). This indicated that intermediates generated from antipyrine aqueous solution degradation by ferrioxalate assisted UV-A-LED photo-Fenton reaction were refractory towards hydroxyl radicals. This is in agreement with our previous study about 50 mg L^{-1} antipyrine solution mineralization under a sono-photo-Fenton process where the main oxidative intermediate species was also hydroxyl radical [30] and the residual TOC was 6.1 mg L^{-1}. In this ferrioxalate UV-A-LED system, where mineralization was mainly attributed to hydroxyl radicals, as will be explained below, different intermediates such as 2-butenedioic acid, butanedioic acid, 4-oxo-pentanoic acid, acetate and formate can be formed in the last step of reaction. These compounds cannot be degraded by $HO^{\bullet}$ radicals or their reaction is very slow, as previously reported [31].

With respect to dissolved oxygen, once the reaction began, dissolved oxygen quickly decreased to below 1.5 mg L^{-1} during the first 20 min. After that, dissolved oxygen slowly increased to 2 mg L^{-1} and then it remained constant. It could be explained because the photolysis of ferrioxalate generates oxalyl radical anion, $C_2O_4^{\bullet-}$, which subsequently undergoes a rapid decarboxylation to form a carbon dioxide radical anion, $CO_2^{\bullet-}$, which consumes oxygen [32].

$$C_2O_4^{\bullet-} \rightarrow CO_2 + CO_2^{\bullet-} \quad (11)$$

$$CO_2^{\bullet-} + O_2 \rightarrow CO_2 + O_2^{\bullet-} \quad (12)$$

On the other hand, hydroxyl radical generated from ferrioxalate photochemistry reacts with organic molecule to form radicals, $R^{\bullet}$, that consumes oxygen generating peroxo-organic radicals, $ROO^{\bullet}$ [33].

$$HO^{\bullet} + RH \rightarrow R^{\bullet} \quad (13)$$

$$R^{\bullet} + O_2 \rightarrow ROO^{\bullet} \quad (14)$$

The small increase of dissolved oxygen above 20 min could be due to the higher importance of oxygen generation by Eq (9) and decomposition of peroxide into water and oxygen.

3.6 Investigation of the free radical mechanism in the ferrioxalate assisted UV-A-LED photo-Fenton system

In order to explain the probable contribution of hydroxyl radicals in this treatment, the degradation of antipyrine was evaluated either in the absence or in the presence of appropriate quenchers of $HO^{\bullet}$. Quenching studies were performed by adding a radical scavenger such as tert-butyl alcohol and methanol. $HO^{\bullet}$ reacts slightly faster with methanol than with tert-butyl alcohol according to Eqs (15) and (16), respectively [34, 35]

$$HO^{\bullet} + CH_3OH \rightarrow H_2O + {}^{\bullet}CH_2OH \qquad (9.7 \times 10^8\ M^{-1}\ s^{-1}) \qquad (15)$$

$$HO^{\bullet} + (CH_3)_3COH \rightarrow {}^{\bullet}CH_2(CH_3)_2COH + H_2O \quad (3.8\text{-}7.6) \times 10^8\ M^{-1}\ s^{-1}) \qquad (16)$$

Fig. 6 shows the antipyrine abatement curve under the optimal operating conditions in the presence and absence of 1M tert-ButOH/Methanol. As it can be seen, the degradation of antipyrine in the presence of both scavengers was practically negligible, indicating that mainly hydroxyl radicals were involved in the degradation reaction. At the beginning of the reaction with tert-butyl alcohol, we can see a slight increase in the degradation because the reaction rate between the HO$^{\bullet}$ and tert-butyl alcohol is lower than with methanol, and so the hydroxyl radical is slower in being scavenged, as indicated above.

Fig. 6 also shows the evolution of dissolved oxygen concentration when methanol or tert-butyl alcohol were added. A quick decrease of oxygen was observed at the beginning while antipyrine concentration decreased by HO$^{\bullet}$ not scavenged during the first 4 min, as indicated above. Once hydroxyl radical availability was totally reduced by alcohols and degradation of antipyrine was ceased, the concentration of dissolved oxygen continuously increased up to values close to saturation by Eq (9) and decomposition of peroxide into water and oxygen.

4. CONCLUSIONS

Intensification of UV-A-LED photo-Fenton reaction with ferrioxalate complexes showed promising results in the elimination of antipyrine as a model compound of emerging pollutants. The iron/oxalic acid molar ratio plays an important role on degradation and mineralization of antipyrine solutions, being 3 the optimal ratio. Under the optimal operating conditions ($[H_2O_2]_o$= 100 mg L^{-1}, $[Fe]_o$= 20 mg L^{-1} and $[H_2C_2O_4]_o$= 100 mg L^{-1}, pH= 2.8, T=24-26ºC] the complete degradation of antipyrine and 93% TOC removal were reached in 2.5 and 60 min, respectively. Antipyrine degradation kinetics follows a pseudo-first-order model. Hydroxyl radicals were found to be the main responsible species in the reaction. In the last step of reaction, different generated intermediates cannot be degraded by $HO^{\bullet}$ radicals or their reaction is very slow. This ferrioxalate-mediated system reduces the amount of H_2O_2 needed (100 mg L^{-1}) for antipyrine degradation and persulfate was not necessary because it could not be activated with UV-A LED nor with Fe^{2+} since it is quickly converted to Fe^{3+} which did not react with persulfate but formed ferrioxalate complexes.

This ferrioxalate-photochemistry-based UV-A-LED oxidation system is a potential alternative to degrade wastewater containing emerging contaminants such as antipyrine.

5. ACKNOWLEDGEMENTS

Financial support from MINECO (CTM2013-44317-R) is gratefully acknowledged.

6. REFERENCES

[1] A. Aguinaco, F.J. Beltrán, J.F. García Araya, A. Oropesa, Photocatalytic ozonation to remove the pharmaceutical diclofenac from water: influence of variables, Chem. Eng. J. 189 (2012) 275.282.

[2] P.H. Roberts, K.V. Thomas, The occurrence of selected pharmaceuticals in wastewater effluent and surface waters of the lower Tyne catchment, Sci. Tot. Environ. 356 (2006) 143-153.

[3] I. Sires, E. Brillas, Remediation of water pollution caused by pharmaceutical residues based on electrochemical separation and degradation technologies: a review, Environ. Int. 40 (2012) 212-229.

[4] S. Khan, L. Aijun, S. Zhang, Q. Hu, Y.-G. Zhu, Accumulation of polycyclic aromatic hydrocarbons and heavy metals in lettuce grown in the soils contaminated with long-term wastewater irrigation, J. Hazard. Mater. 152 (2008) 506-515.

[5] J.L. Santos, I. Aparicio, M. Callejón, E. Alonso, Occurrence of pharmaceutically active compounds during 1-year period in wastewaters from four wastewater treatment plants in Seville (Spain)., J. Hazard. Mater. 164 (2009) 1509-1516.

444 [6] M. Petrovi´c, M.D. Hernando, M.S. Diaz-Cruz, D. Barcelo, Liquid chromatography-
445 tandem mass spectrometry for the analysis of pharmaceutical residues in environmental
446 samples: a review, J. Chromatogr. A. 1067 (2005) 1–14.

447

448 [7] S. Zuhlke, U. Dunnbier, T. Heberer, Detection and identification of phenazone-type
449 drugs and their microbial metabolites in ground and drinking water applying solid-phase
450 extraction and gas chromatography with mass spectrometric detection, J. Chromatogr. A.
451 1050 (2004) 201–209.

452

453 [8] T. Deblonde, C. Cossu-Leguille, P. Hartemann, P. Emerging pollutants in wastewater:
454 a review of the literature, Int. J. Hyg. Environ. Health. 214 (2011) 442-8.

455

456 [9] L. W. Matzek, K.E. Carter, Activated persulfate for organic chemical degradation: A
457 review, Chemosphere, 151 (2016) 178-188.

458

459 [10] F. Yuan, C. Hu, X. Hu, J. Qu, M. Yang, Degradation of selected pharmaceuticals in
460 aqueous solution with UV and UV/H_2O_2, Wat. Res. 43 (2009) 1766-1774.

461

462 [11] C. Tan, N. Gao, Y. Deng, Y. Zhang, M. Sui, J. Deng, Degradation of antipyrine by
463 UV, UV/H_2O_2 and UV/PS, J. Hazard. Mater. 260 (2013) 1008-1016.

464

[12] A. Durán, J.M. Monteagudo, I. Sanmartin, A. García-Díaz, Sonophotocatalytic mineralization of antipyrine in aqueous solution, Appl. Catal. B: Environ. 138 (2013) 318-325.

[13] A. Durán, J.M. Monteagudo, I. Sanmartin, A. Carrasco, Solar photo-Fenton mineralization of antipyrine in aqueous solution, J. Environ. Manage 130 (2013) 64-71.

[14] A. Durán, J.M. Monteagudo, I. Sanmartin, A. Valverde, Solar photodegradation of antipyrine in a synthetic WWTP effluent in a semi-industrial installation, Sol. Energy Mat. Sol. C. 125 (2014) 215-222.

[15] C. Tan, N. Gao, Y. Deng, W. Rong, S. Zhou, N. Lu, Degradation of Antipyrine by Heat Activated Persulfate, Sep. Purif. Technol 109 (2013) 122-128.

[16] K. Natarajan, T.S. Natarajan, H.C. Bajaj, R.J. Tayade, Photocatalytic reactor based on UV-LED/TiO_2 coated quartz tube for degradation of dyes, Chem. Eng. J. 178 (2011) 40-49.

[17] M. Rasoulifard, M. Fazli, M. Eskandarian, Kinetic study for photocatalytic degradation of Direct Red 23 in UV-LED/nano-TiO_2/$S_2O_8^{2-}$ process: Dependence of degradation kinetic on operational parameters, J. Ind. Eng. Chem. 20 (2014) 3695- 3702.

[18] W. Wen-Yu, K. Young, Photocatalytic degradation of reactive red 22 in aqueous solution by UV-LED radiation, Wat.Res. 40 (2006) 2249-2258.

[19] S. Malato, J. Blanco, M.I. Maldonado, P. Fernández, D. Alarcón, M. Collares, J. Farinha, J. Correia de Oliveira, Engineering of solar photocatalytic collectors, Solar Energy 77 (2004) 513-524.

[20] R. Bauer, G. Waldner, H. Fallmann, S. Hager, H. Karé, T. Krutzler, S. Malato, P. Maletzky, The photo-Fenton reaction and the TiO_2/UV process for wastewater treatment-novel developments, Catal. Today 53 (1999) 131-144.

[21] A. Safarzadeh-Amiri, J.R. Bolton, S.R. Cater, Ferrioxalate-mediated photodegradation of organic pollutants in contaminated water, Wat. Res. 31 (1997) 787-798.

[22] K. Selvam, M. Muruganandham, M. Swaminathan, Deposition of highly photoconductive wide band gap a-SiOx:H thin films at a high temperature without H_2-dilution, Sol. Energy Mater. Sol. Cells 89 (2005) 61-74.

[23] J.M. Monteagudo, A. Durán, R. González, A.J. Expósito, In situ chemical oxidation of carbamazepine solutions using persulfate simultaneously activated by heat energy, UV light, Fe^{2+} ions, and H_2O_2, Appl. Catal. B: Environ. 176 (2015) 120-129.

510 [24] C. Liang, C-F Huang, N. Mohanty, R. M. Kurakalvaa, A rapid spectrophotometric
511 determination of persulfate anion in ISCO, Chemosphere, 73 (2008) 1540-1543.
512
513 [25] D.P. Morgan, C.L. Scofield, Neural Networks and Speech Processing. Kluwver
514 Academic Publishers. London, 1991.
515
516 [26] R Nath, B Rajagopalan, R Ryker, Determining the saliency of input variables in
517 neural network classifiers, Comput. Oper. Res. 24 (1997) 767-773.
518
519 [27] J.M. Monteagudo, A. Durán, R. Culebradas, I. San Martin, A. Carnicer, Optimization
520 of pharmaceutical wastewater treatment by solar/ferrioxalate photo-catalysis, J. Environ.
521 Manage 128 (2013) 210-219.
522
523 [28] B.M. Souza, M.W.C. Dezotti, R.A.R. Boaventura, V.J.P. Vilar, Intensification of a
524 solar photo-Fenton reaction at near neutral pH with ferrioxalate complexes: A case study
525 on diclofenac removal from aqueous solutions, Chem. Eng. J. 256 (2014) 448-457.
526
527
528 [29] G. V. Buxton, C.L. Grennstock, W.P. Helman, A.B. Ross, Critical Review of rate
529 constants for reactions of hydrated electrons, hydrogen atoms and hydroxyl radicals
530 (·OH/·O−) in Aqueous Solution, J. Phys. Chem. Ref. Data 17 (1988) 513-886.
531

[30] J.M. Monteagudo, A. Durán, A. Fernández, A. Carnicer, J.M. Frades, M.A. Alonso, Proceedings of the 13th Mediterranean Congress in Chemical Engineering, Barcelona, 2014.

[31] J.M. Monteagudo, A. Durán, J. Latorre, A.J. Expósito, Application of activated persulfate for removal of intermediates from antipyrine wastewater degradation refractory towards hydroxyl radical, J. Hazard. Mater. 306 (2016) 77-86.

[32] H.-P. Chenga, Y.-H. Huanga, C. Leeb, Decolorization of reactive dye using a photo-ferrioxalate system with brick grain-supported iron oxide, J. Hazard. Mater. 188 (2011) 357-362.

[33] S. Miralles-Cuevas, L. Prieto-Rodríguez, E. De Torres-Socías, M.I. Polo-López, P. Fernández-Ibañez, I. Oller, S. Malato, Strategies for hydrogen peroxide dosing based on dissolved oxygen concentration for solar photo-Fenton treatment of complex wastewater, Global Nest J. 16 (2014) 553-560.

[34] R. Matta, S. Tlili, S. Chiron, S.Barbati, Removal of carbamazepine from urban wastewater by sulfate radical oxidation, Removal of carbamazepine from urban wastewater by sulfate radical oxidation, Environ. Chem. Lett. 9 (2011) 347-353.

[35] G.P. Anipsitakis, D.D. Dionysiou, Radical generation by the interaction of transition metals with common oxidants, Environ. Sci. Technol. 38 (2004) 3705-3712.

Figure captions:

Figure 1: Structure and properties of antipyrine.

Figure 2: Schematic diagram of UV-LED reactor (1: magnetic stirrer, 2: stirring bar, 3: glass reactor, 4: quartz plate, 5: LED emitter, 6: heat sink, 7: cable connection to DC power supply).

Figure 3: Degradation of Antipyrine aqueous solution in a UV-A LED photo-Fenton system intensified by ferrioxalate and with addition of persulfate. Reaction time: 60 min, temperature= 24-26ºC. a) Effects of initial concentrations of Fe^{2+} and $S_2O_8^{2-}$; b) Effects of initial concentrations of Fe^{2+} and H_2O_2; c) Effects of initial concentrations of H_2O_2 and $H_2C_2O_4$; d) Effects of initial concentrations of Fe^{2+} and $H_2C_2O_4$. [a,b,c: Center point operating conditions; d: Optimal operating conditions].

Figure 4: Mineralization of antipyrine aqueous solution in a UV-A LED photo-Fenton system intensified by ferrioxalate and with addition of persulfate. Reaction time: 60 min, temperature= 24-26ºC. a) Effects of initial concentrations of Fe^{2+} and $S_2O_8^{2-}$; b) Effects of initial concentrations of Fe^{2+} and H_2O_2; c) Effects of initial concentrations of H_2O_2 and $H_2C_2O_4$; d) Effects of initial concentrations of Fe^{2+} and $H_2C_2O_4$. [a,b,c: Center point operating conditions; d: Optimal operating conditions].

Figure 5: Evolution of antipyrine, TOC and dissolved oxygen concentrations along the reaction under the optimal operating conditions: ($[H_2O_2]_o$= 100 mg L^{-1}, $[Fe^{2+}]_o$= 20 mg L^{-1}, $[H_2C_2O_4]_o$= 100 mg L^{-1}, $[S_2O_8^{2-}]_o$= 0 mg L^{-1}, temperature= 24-26ºC, pH= 2.8).

570

571 **Figure 6:** Antipyrine and TOC abatement and dissolved oxygen curves under the optimal

572 operating conditions in the presence and absence of 1M tert-ButOH/Methanol. Operating

573 conditions: ($[H_2O_2]_o$= 100 mg L^{-1}, $[Fe^{2+}]_o$= 20 mg L^{-1}, $[H_2C_2O_4]_o$= 100 mg L^{-1}, $[S_2O_8^{2-}]_o$=

574 0 mg L^{-1}, temperature= 24-26ºC, pH= 2.8).

575

576

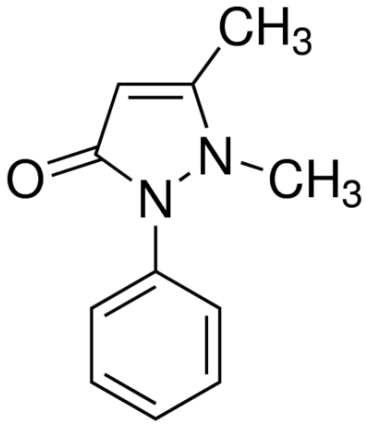

Molecular structure

Formula: $C_{11}H_{12}N_2O$

Molecular weight: 188.23 g mol^{-1}

587

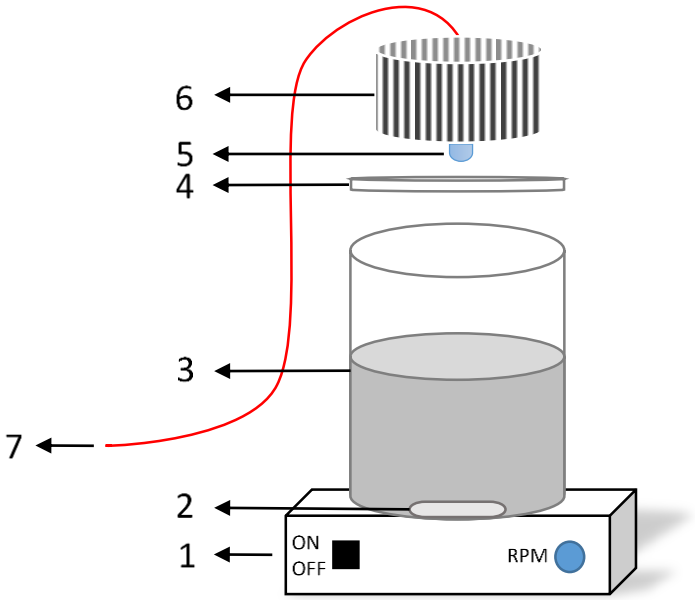

588

589

590

591

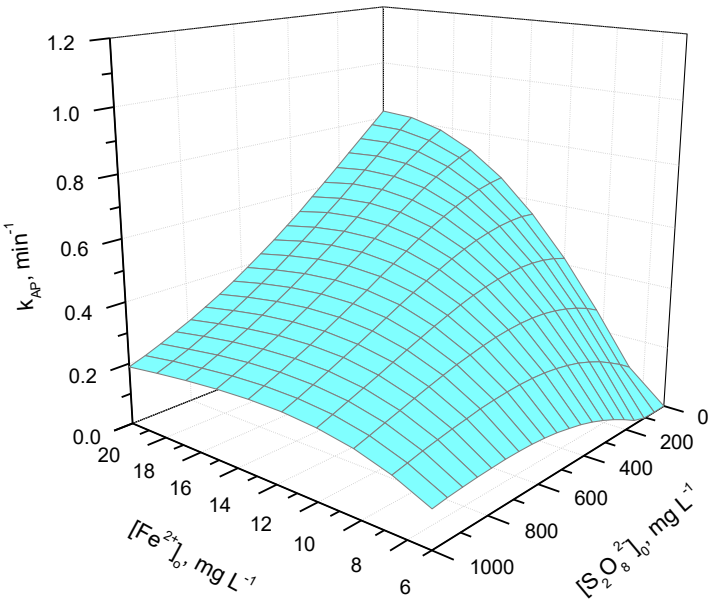

592

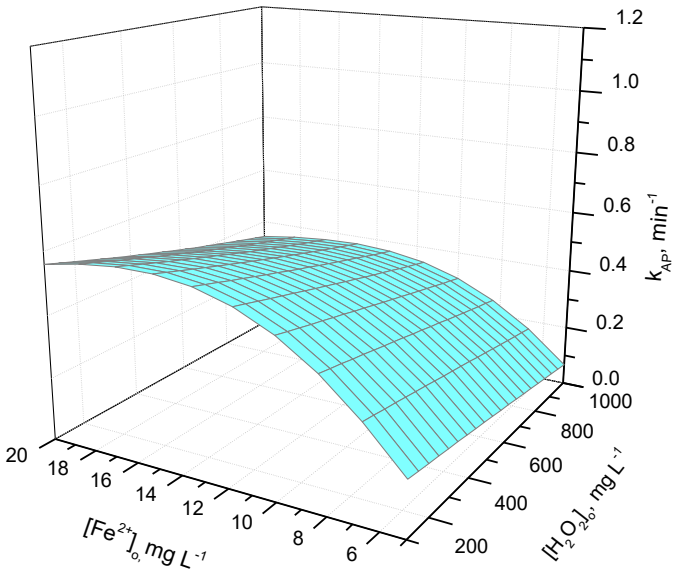

593
594
595 a)
596 b)

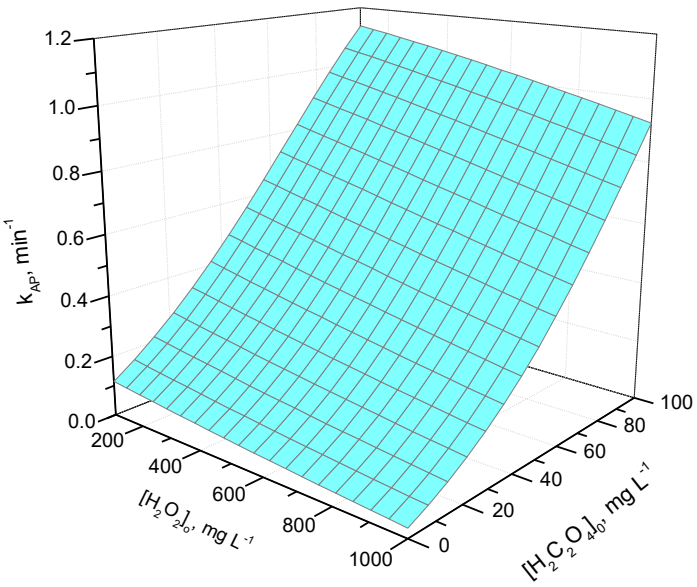

597

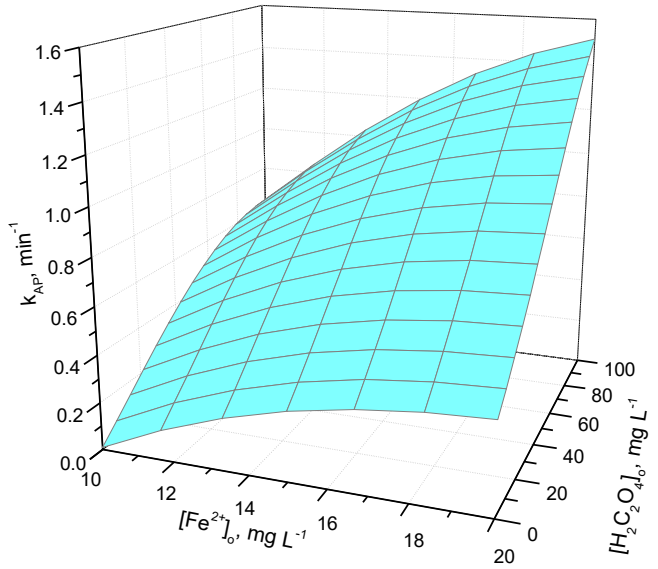

598
599 c)
600 d)
601

602 **Figure 3.**

603

604

605

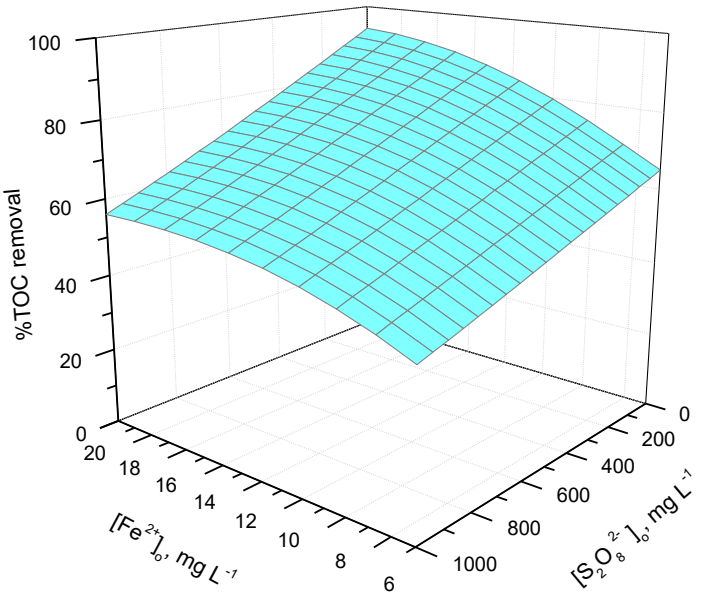

606

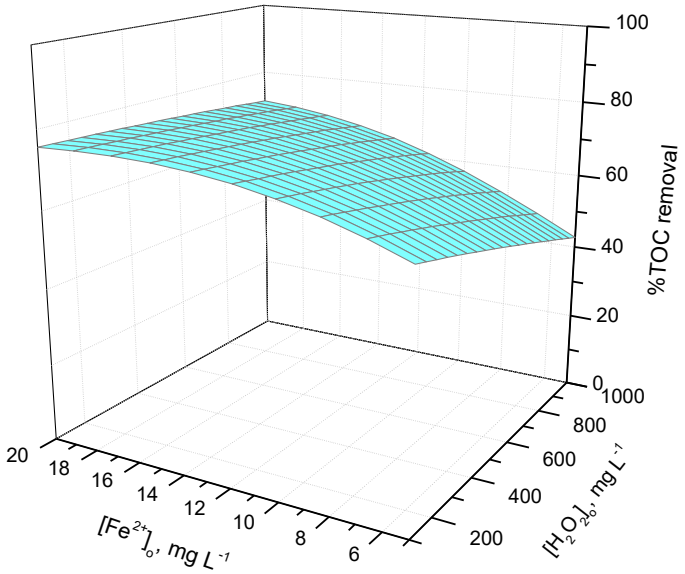

607
608
609 a)
610 b)

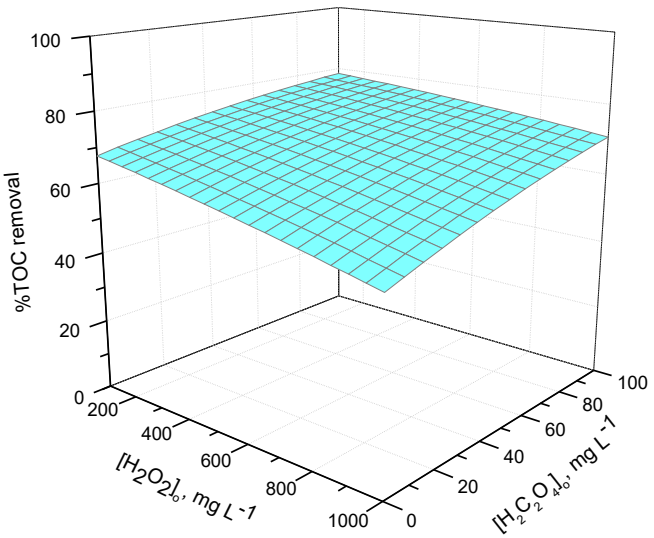

611

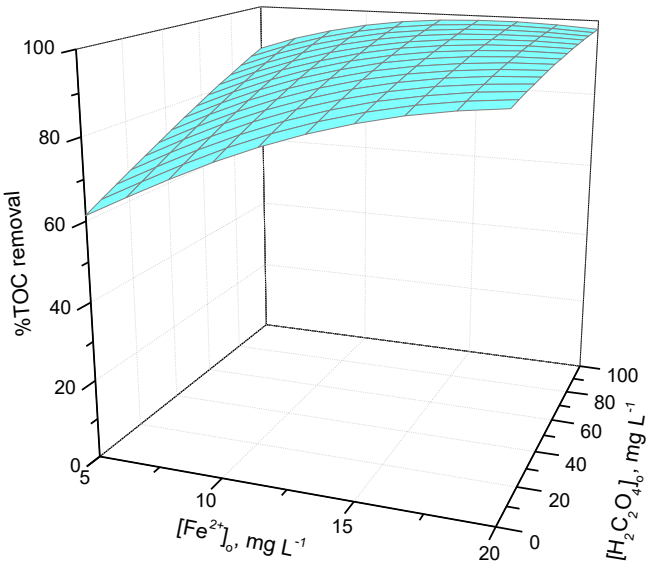

612
613 c)
614 d)
615 **Figure 4.**

616

617

618

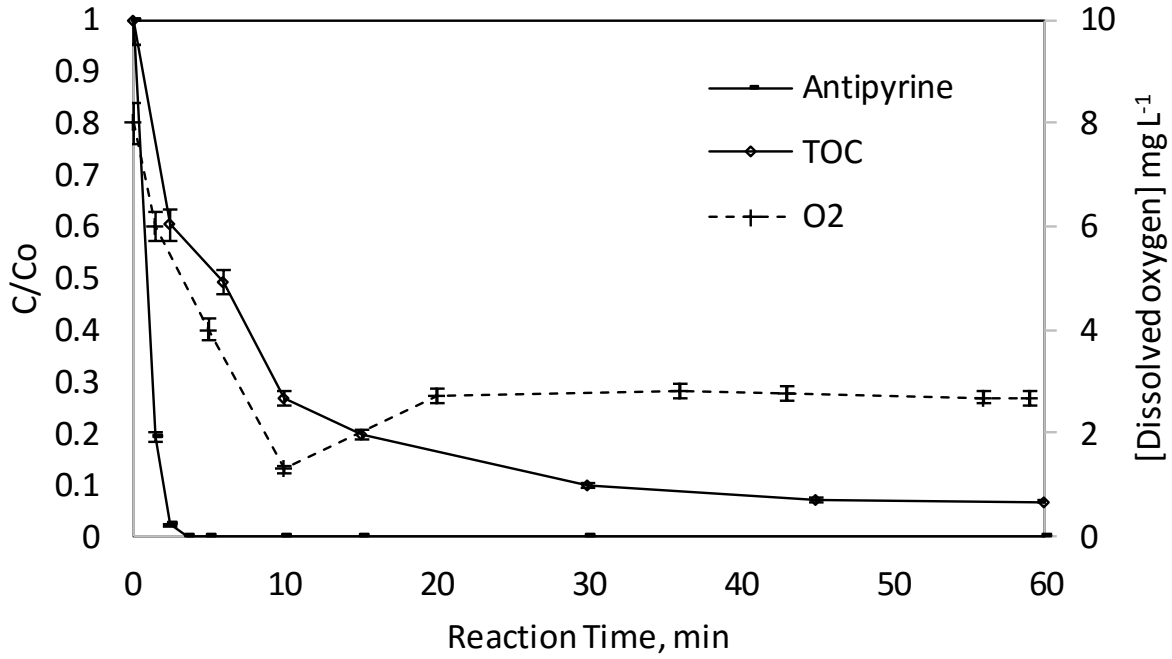

619
620
621
622
623 **Figure 5.**

624

625

626

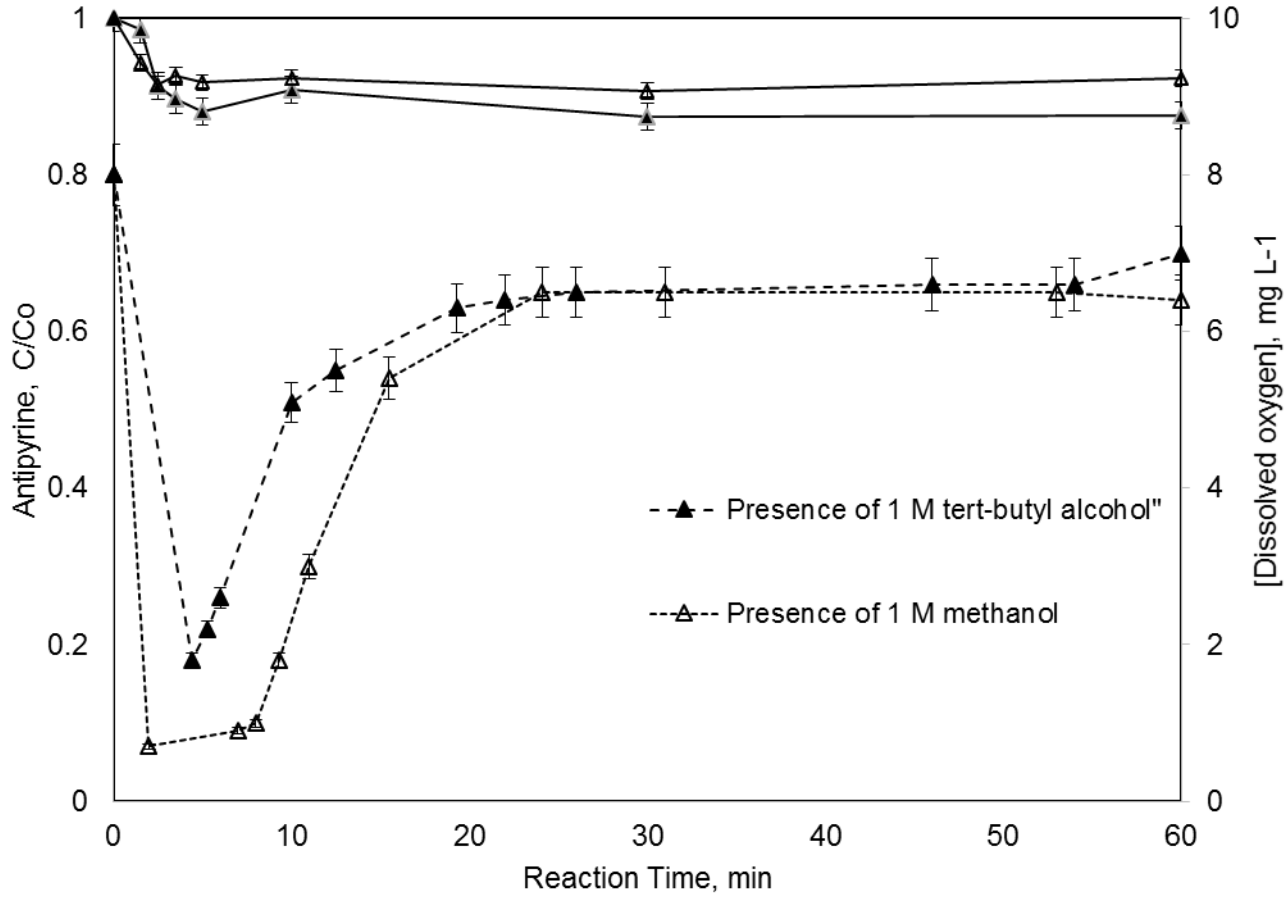

628
629
630
631 **Figure 6.**

632

633

Table 1. The 4-factor Central Composite Experimental Design Matrix. Degradation and mineralization of an Antipyrine aqueous solution by UV-LED photo-Fenton intensified by ferrioxalate with addition of persulfate. $[TOC]_0$= 35 mg L^{-1}; pH: 2.8; UV-A LED lamp (11 W; λ= 365 nm).

FACTORIAL DESIGN					*Response Functions*	
Experiment	**$[H_2O_2]_o$, mg L^{-1}**	**$[Fe(II)]_o$, mg L^{-1}**	**$[H_2C_2O_4]_o$, mg L^{-1}**	**$[S_2O_8^{2-}]_o$, mg L^{-1}**	**k_{AP}, min^{-1}**	**Mineralization degree, %**
1	775	16.25	75	750	0.500	62.33
2	325	16.25	75	750	0.612	66.92
3	775	8.75	75	750	0.487	57.05
4	325	8.75	75	750	0.595	63.11
5	775	16.25	25	750	0.233	62.51
6	325	16.25	25	750	0.202	67.02
7	775	8.75	25	750	0.083	46.56
8	325	8.75	25	750	0.120	58.93
9	775	16.25	75	250	0.895	82.37
10	325	16.25	75	250	1.060	86.59
11	775	8.75	75	250	0.455	70.99
12	325	8.75	75	250	0.672	82.30
13	775	16.25	25	250	0.291	75.82
14	325	16.25	25	250	0.377	79.92
15	775	8.75	25	250	0.112	63.41
16	325	8.75	25	250	0.154	73.63
17	1000	12.5	50	500	0.349	64.35
18	100	12.5	50	500	0.346	67.95
19	550	20	50	500	0.551	74.07
20	550	5	50	500	0.123	51.73
21	550	12.5	100	500	1.040	74.87
22	550	12.5	0	500	0.067	57.62
23	550	12.5	50	1000	0.403	60.11
24	550	12.5	50	0	0.612	81.86
25	550	12.5	50	500	0.432	63.38
26	550	12.5	50	500	0.431	63.80
27	550	12.5	50	500	0.431	63.54
Coded levels		Natural levels				
(+α)	1000	20	100	1000		
(-α)	100	5	0	0		
(+1)	775.00	16.25	75.00	750.00		
(-1)	325.00	8.75	25.00	250.00		
(0)	550	12.5	50	500		
ADDITIONAL EXPERIMENTS						
28[a]	100	20	100	0	1.51	93.00
29[b]	100	20	100	0	0.016	-
30[c]	100	20	100	0	0.028	-

[a]: Optimal conditions

[b]: Optimal conditions in the presence of methanol

[c]: Optimal conditions in the presence of tert-butyl alcohol

Table 2. Equation and parameters of Neural Network fittings for the two Response Funstions: 1) pseudo-first order kinetic rate constant of antipyrine degradation 2) Mineralization Degree of Antipyrine aqueous solution. UV-A LED photo-Fenton system intensified by ferrioxalate with persulfate addition.

Equation*

Response Function = $N_1 \times (1/(1+1/EXP([H_2O_2]_o) \times W_{11} + ([Fe(II)]_o) \times W_{12} + ([H_2C_2O_4]_o) \times W_{13} + ([S_2O_8^{2-}]_o) \times W_{14}))) + N_2 \times (1/(1+1/EXP([H_2O_2]_o) \times W_{21} + ([Fe(II)]_o) \times W_{22} + (([H_2C_2O_4]_o) \times W_{23} + (([S_2O_8^{2-}]_o) \times W_{24} +)))$

Weight factors	Parameter	Values of neurons and factors	
		$k_{AP,}$ min^{-1}	%TOC removal
N_1	**Neuron**	**-3.6600**	**-1.3037**
W_{11}	$[H_2O_2]_o$	-0.3770	0.7156
W_{12}	$[Fe(II)]_o$	-2.4656	-2.066
W_{13}	$[H_2C_2O_4]_o$	0.7370	-1.026
W_{14}	$[S_2O_8^{2-}]_o$	-1.9863	-0.832
N_2	**Neuron**	**2.7738**	**2.5320**
W_{21}	$[H_2O_2]_o$	-0.5871	0.024
W_{22}	$[Fe(II)]_o$	-1.1411	-0.3002
W_{23}	$[H_2C_2O_4]_o$	2.2131	-0.0696
W_{24}	$[S_2O_8^{2-}]_o$	-2.0302	-0.8043

* Parameter values in equation must be previously normalized to the (0.1) interval

Saliency analysis of the input variables for the neural network (%).

	Parameters			
Neural network output	$[H_2O_2]_o$	$[Fe(II)]_o$	$[H_2C_2O_4]_o$	$[S_2O_8^{2-}]_o$
k_{AP}, min^{-1}	8.30	31.70	25.15	34.84
%TOC removal	8.74	34.78	13.97	42.52

Appendix A. Supplementary Information

Degradation and Mineralization of Antipyrine by UV-A LED Photo-Fenton Reaction Intensified by Ferrioxalate with Addition of Persulfate

Konstantina Davididou[a], José María Monteagudo[b,*], Efthalia Chatzisymeon[a], Antonio. Durán[b], Antonio José Expósito[b]

[a] *Institute for Infrastructure and Environment, School of Engineering, The University of Edinburgh, Edinburgh EH9 3JL, United Kingdom.*

[b] *Department of Chemical Engineering, Grupo IMAES, Escuela Técnica Superior de Ingenieros Industriales, Instituto de Investigaciones Energéticas y Aplicaciones Industriales (INEI) University of Castilla-La Mancha, Avda. Camilo José Cela 3, 13071 Ciudad Real (Spain).*

* To whom correspondence should be addressed

Fax: 0034 926295361.
Phone: 0034 926295300, ext: 3888
email: josemaria.monteagudo@uclm.es

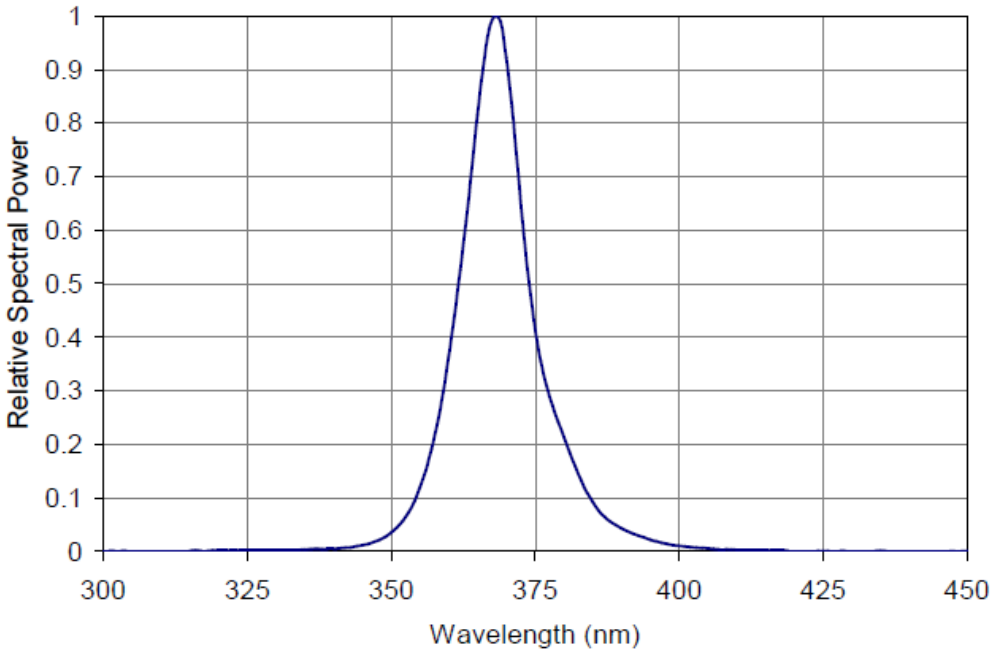

Fig. S1: Typical Relative Spectral Power Distribution

Table S1. Preliminary study of degradation of an Antipyrine aqueous solution by UV-LED photo-Fenton intensified by ferrioxalate with addition of persulfate. $[TOC]_o$= 35 mg L^{-1}; pH: 2.8; UV-A LED lamp (11 W; λ= 365 nm).

Preliminary study					
Experiment	**$[H_2O_2]_o$, mg L^{-1}**	**$[Fe(II)]_o$, mg L^{-1}**	**$[H_2C_2O_4]_o$, mg L^{-1}**	**$[S_2O_8^{2-}]_o$, mg L^{-1}**	**k_{AP}, min^{-1}**
P-1	100	12.5	50	500	0.346
P-2	90	12.5	50	500	0.302
P-3	70	12.5	50	500	0.248
P-4	50	12.5	50	500	0.113
P-5	20	12.5	50	500	0.014

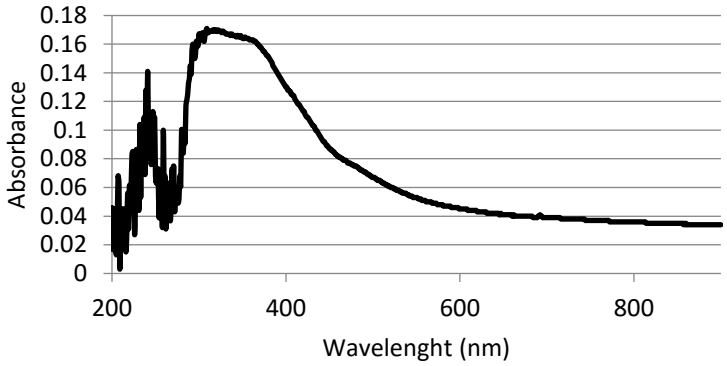

Figure S2: Absorption spectra of ferrioxalate solution

764
765
766
767

768